Available online at www.sciencedirect.com
ScienceDirect
Biochemical and Biophysical Research Communications 349 (2006) 24–30
BBRC
www.elsevier.com/locate/ybbrc

Fluorescence lifetime imaging microscopy (FLIM) detects stimulus-dependent phosphorylation of the low density lipoprotein receptor-related protein (LRP) in primary neurons

Ithan D. Peltan [a], Anne V. Thomas [a], Irina Mikhailenko [b], Dudley K. Strickland [b], Bradley T. Hyman [a,*], Christine A.F. von Arnim [a,c]

[a] *Alzheimer's Disease Research Unit, Massachusetts General Hospital, Harvard Medical School, Charlestown, MA 02129, USA*
[b] *Center for Vascular and Inflammatory Diseases, University of Maryland School of Medicine, Baltimore, MD 21201, USA*
[c] *Department of Neurology, Ulm University, 89081 Ulm, Germany*

Received 14 July 2006
Available online 14 August 2006

Abstract

The low-density lipoprotein receptor-related protein (LRP) is a large, endocytic receptor involved in intracellular signalling. LRP acts as a co-receptor with the PDGF-receptor (PDGF-r) for platelet-derived growth factor (PDGF). PDGF-r and Src-kinases induce tyrosine-phosphorylation of LRP. We used fluorescence lifetime imaging microscopy (FLIM) to specifically detect LRP phosphorylation, measure its extent and localization in intact cells, and assess its effects upon LRP–APP interaction. Robust phosphorylation of LRP throughout the cell was observed after overexpression of Src-kinase. This depended on LRP's distal NPXY domain. By contrast, activation of the PDGF-r resulted in phosphorylation of the subpopulation of LRP at or near the cell surface. PDGF activation triggered phosphorylation of endogenous LRP in primary neurons. LRP is also a trafficking receptor for the Alzheimer-related molecule amyloid-precursor-protein (APP). PDGF stimulation did not affect LRP–APP interactions. This approach allows exquisite subcellular resolution of specific LRP post-translational changes and protein-protein interactions of endogenous proteins in intact cells.

Keywords: LRP; Phosphorylation; FLIM; FRET; PDGF; APP

The low-density lipoprotein (LDL) receptor-related protein (LRP) was initially recognized as an endocytic receptor for apolipoprotein E (ApoE)-enriched lipoproteins and α_2-macroglobulin (α_2M). The single-chain precursor of LRP is cleaved in the *trans*-Golgi compartment by a furin-like protease to generate 515 kDa extracellular α-subunit (heavy chain) and an 85 kDa β-chain containing the transmembrane domain and a short cytoplasmic tail. Mature LRP exists as a non-covalently associated heterodimer of these two subunits strongly expressed in neurons, hepatocytes and other cell types [1]. Ligand-binding domains within the heavy chain mediate endocytosis of a large number of structurally and functionally diverse ligands, ranging from lipoproteins to proteinases to bacterial toxins (for review see [2]).

Mounting evidence also points to functions for LRP in signal transduction events. ApoE binding to LRP inhibits the migration of vascular smooth muscle cells triggered by platelet-derived growth factor (PDGF) and LRP deficiency results in atherosclerogenic disregulation of the PDGF-receptor (PDGF-r) [3–5]. Treatment of cells with PDGF-BB causes transient tyrosine phosphorylation of LRP's second NPXY motif in its intracellular domain (ICD) [6,7]. Following PDGF stimulation, PDGF-r-β and LRP are closely associated in coated pits and endosomal compartments independent of growth

* Corresponding author. Fax: +1 617 724 1480.
E-mail address: bhyman@partners.org (B.T. Hyman).

0006-291X/$ - see front matter © 2006 Elsevier Inc. All rights reserved.
doi:10.1016/j.bbrc.2006.07.212

factor binding to LRP. In the absence of PDGF-r-β activation, LRP can be phosphorylated by constitutively active Src [8].

Finally, LRP has been implicated in trafficking and metabolism of the Alzheimer related protein APP. LRP interaction with APP occurs via both extracellular (via APP's KPI domain) and intracellular protein interaction via NPXY domains and adapter proteins like FE65 [9].

Phosphorylation of the NPXY domain could therefore alter LRP function in important ways. We recently reported that the serine and threonine phosphorylation state of the LRP-ICD influences both tyrosine phosphorylation and LRP's affinity for cytosolic adaptors [10]. Given the complex set of interactions of LRP with co-receptors at that cell surface on the one hand and with trafficking and recycling of cargos like APP in ER, Golgi, and endosomal compartments, there is a need for a better understanding of the cellular localization of post-translational regulatory events like phosphorylation. Here, we develop a fluorescence resonance energy transfer (FRET)-based technique, FLIM, to determine where in the cell and in response to which stimulus LRP tyrosine phosphorylation occurs. Since both PDGF and an inhibitor of PDGF-r signalling have recently been shown to influence APP processing [11–13], we were additionally interested to learn if LRP phosphorylation induced by PDGF-r activation alter LRP's interaction with APP.

Materials and methods

Proteins, antibodies, and expression constructs. Since full-length LRP is difficult to express due to its large size, we transfected cells with LRP mini-receptors. We utilized a previously described expression construct encoding the LRP light chain (LRPβ) and a small portion of the heavy chain (amino acids 3844-4525) with two myc tags at the N-terminus (myc-LRPβ) or C-terminus (LRPβ-myc) [7]. NPXY domain mutations were introduced at the first (NPTY → APTA) or second (NPVY → APVA) NPXY motif with the QuikChange kit (Stratagene, La Jolla, CA). Construction of mLRP1, which includes LRP's first ligand-binding domain N-terminal to LRPβ-myc, has been previously described [14]. The cDNA for APP695 was inserted into the BamHI and SacII sites of the pcDNA3.1/V5-His-TOPO vector (Invitrogen, Carlsbad, CA) to make APP695-V5. Constructs encoding cDNA for PDGF-r-β and the Src variants in pUseAmp as well as the pUseAmp empty vector were from Upstate (Lake Placid, NY). The authenticity of all constructs was verified by sequencing.

Antibodies against phosphotyrosine, the myc epitope, and Src were purchased from Upstate. Mouse anti-V5 epitope was from Invitrogen. A hybridoma secreting a mouse antibody to the LRP-ICD domain (11H4) was obtained from the ATCC (Rockville, MD). C8 rabbit polyclonal antibody against the APP-C-terminus was a generous gift of D. Selkoe (Brigham and Women's Hospital, Boston, MA). PDGF-r-β was detected with a polyclonal rabbit antibody against its C-terminus (Santa Cruz Biotechnology, Santa Cruz, CA). Jackson Immunoresearch (West Grove, PA) supplied antibodies conjugated to FITC and Cy3 and Rockland (Gilbertsville, PA) provided antibodies conjugated to IRDye700 and IRDye800. Alexa488 conjugated antibodies were from Molecular Probes (Eugene, OR). PDGF-BB was obtained from R&D Systems (Minneapolis, MN).

Cell culture and transient transfection. Mouse neuroblastoma N2a cells were maintained in OPTI-MEM (Gibco, Grand Island, NY) supplemented with 5% fetal bovine serum (FBS). WI-38 lung fibroblasts from the ATCC (www.atcc.org) were maintained in Dulbecco's modified Eagle's medium (Gibco) with 10% FBS. Transient transfection was performed one day after passaging using Fugene 6 according to manufacturer's instructions (Roche, Indianapolis, IN). Primary neurons were generated from CD1 mice at embryonic day 15–16 as described [15]. The embryonic cortices, including hippocampus, were dispersed in neurobasal media (NBM, Gibco) containing 10% FBS. Four-well glass slides were coated with 0.1 mg/ml poly-L-lysine for 1 h, washed twice with phosphate-buffered saline (PBS), and air dried before neurons were plated. Cells were incubated in 5% CO_2 at 37 °C for 1 h before FBS media was replaced with NBM containing 1X B-27.

Immunoprecipitation. N2a cells in 100 mm dishes were washed twice with cold PBS and harvested in 0.5% NP-40, 2 mM EDTA, 50 mM Tris–HCl, 150 mM NaCl, 1 mM $NaVO_4$. Immunoprecipitation of myc-tagged proteins was carried out with the μMACS epitope isolation kit (Miltenyi Biotec, Auburn, CA) according to manufacturer's instructions. Specific pull down was demonstrated by the absence of pull down in cells transfected with the prey protein only. Immunoprecipitates and lysates separated on 4–20% tris–glycine gels (Invitrogen) were detected using infrared detection antibodies on a two-channel LI-COR Odyssey infrared imaging system (Lincoln, NE).

Immunocytochemistry. Immunostaining was performed 24–48 h after transfection. After washing once with cold tris-buffered saline (TBS), cells were fixed in 4% paraformaldehyde for 10 min and permeabilized with 0.5% Triton X-100 for 20 min, washing three times with TBS after each step. Cells were then blocked in 1.5% normal goat serum and incubated in primary antibodies in TBS for 1 h at room temperature. After removal of primary antibodies, cells were washed thrice with TBS before fluorophore-conjugated secondary antibodies were applied in TBS for 1 h at room temperature. Slides were washed four times and coverslipped using GVA mounting solution (Zymed, South San Francisco, CA).

Cytokine treatment. Primary neurons were serum starved after 7–10 days in vitro in NBM containing 0.02X B-27 for 48–72 h and then for 2 h in pure NBM [16]. WI-38 cells were serum starved for 48 h in pure DMEM. Cells were treated with 50 ng/ml PDGF-BB in serum-starve media for 12–15 min before immunocytochemistry. TBS wash and fixative were supplemented with 1 mM activated $NaVO_4$.

Fluorescence lifetime imaging microscopy (FLIM). In this study, we developed a FLIM assay to simultaneously assess the effect of a stimulus on the phosphorylation state of LRP and the subcellular localisation of the effect in intact cells. FLIM is a fluorescence resonance energy transfer (FRET)-based assay that allows for the assessment of close proximity between two epitopes [17]. FLIM is based on the observation that the fluorescence lifetime of a donor fluorophore decreases proportionally to R^6 if a FRET acceptor is in close proximity (<10 nm) [15]. To assess the LRP phosphorylation state in response to defined stimuli, donor (either FITC or Alexa 488) and acceptor (Cy3) fluorophores were attached to the LRP ICD and phosphotyrosine epitopes, respectively. Donor fluorophores (FITC, Alexa488) were excited on a two-photon system (Radiance 2000, Bio-Rad, Hercules, CA) at 800 nm by a femtosecond pulse from a mode-locked Ti-sapphire laser (Mai Tai; Spectra-Physics, Mountain View, CA). Emissions filtered with a center of 515 nm were collected by a high-speed photomultiplier tube (MCP R3809; Hamamatsu, Hamamatsu City, Japan) and a fast time-correlated single photon counting acquisition board (SPC 830; Becker and Hickl, Berlin, Germany).

Fluorophore lifetimes were fit to two-exponential decay curves on SpcImage 2.60 (Becker and Hickl, Berlin, Germany). The non-"FRETing" population, measured as the donor lifetime in the absence of an acceptor, was represented as t2; the "FRETing" population (t1) is represented in the figures. Lifetime values represent averages across 12–25 cells from a single experiment; cell images and lifetime distributions are representative examples. Each experiment was repeated at least three times.

Statistical Analysis. Statistical analysis was performed by ANOVA and Fisher's PLSD post-hoc test. Results were considered significant if $p < 0.05$.

Results and discussion

Src kinase leads to phosphorylation of LRP's second NPXY domain predominantly at or near the cell surface

We developed an assay to detect the subcellular distribution of tyrosine phosphorylation of LRP in intact cells. First, we confirmed that activation of Src kinase leads to phosphorylation of LRP's intracellular domain [7,8]. LRPβ-myc immunoprecipitated from N2a cells was highly tyrosine phosphorylated in the presence of constitutively active Src (ca-Src, Fig. 1A). Src coimmunoprecipitated with LRPβ-myc, suggesting that Src directly phosphorylates LRP. To measure LRP phosphorylation in intact N2a cells using FLIM, donor and acceptor fluorophores were attached to the intracellular domain of transfected mLRP1 and to phosphotyrosine epitopes, respectively [18]. A typical LRP staining pattern (FITC, green) and bright, widespread phosphotyrosine staining (Cy3, red) was observed (Fig. 1B). As expected, the lifetime of FITC bound to the LRP-ICD decreased sharply upon cotransfection of mLRP1 with constitutively active Src (ca-Src), indicating close proximity between the LRP-ICD and phosphotyrosine residues. A negative control, cotransfection of dominant negative Src (dn-Src) did not increase the LRP-phosphotyrosine specific signal (Fig. 1C). The small amount of LRP phosphorylation observed in the presence of dn-Src is consistent with studies showing that other tyrosine kinases can act on LRP [19].

Both of LRP's NPXY motifs represent potential sites for tyrosine phosphorylation, but previous studies have identified tyrosine 63 in the motif distal to the membrane as the phosphorylation site for Src [7,19]. We confirmed this finding and the FLIM assay's validity by showing that mutation of tyrosine 63 but not tyrosine 29 of LRPβ to alanine dramatically weakened the amount of FRET detected by the FLIM assay upon co-transfection with ca-Src (Fig. 1C), suggesting that the assay is sensitive to which tyrosine is phosphorylated.

Since the lifetime values can be visualized in a pseudocolored FLIM image, this assay furthermore provides information about the subcellular distribution of epitopes in close proximity. While red and orange pixels indicate "FRETing" molecules, non-"FRETing" molecules are displayed in blue. As is shown in Fig. 1D, Src-induced LRP phosphorylation predominantly occurs at the cell periphery and not in the compartments of highest LRP expression.

PDGF-BB treatment leads to LRP phosphorylation at or near the cell surface in fibroblast and neuronal cells

While serine and threonine phosphorylation of LRP appears to be a constitutive process, phosphorylation of its tyrosine residues occurs transiently in response to extracellular signals [6,7,10,20,21]. Thus, we tested the potential of our FLIM assay to detect smaller changes in the fraction of phosphorylated LRP molecules brought about by a more physiologic stimulus. PDGF-BB is known to trigger transient phosphorylation of LRP via activation of PDGF-r, a process in which LRP seems to act as a coreceptor [8]. We evaluated phosphorylation of endogenous LRP

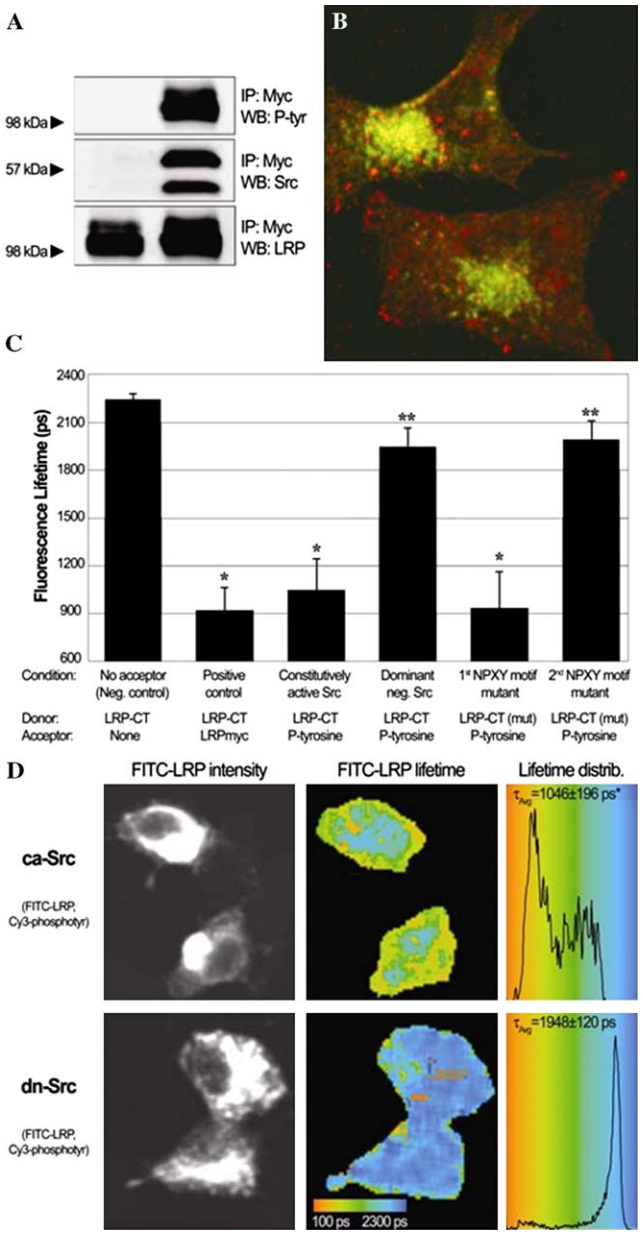

Fig. 1. Src-induced LRP 2nd NPXY phosphorylation. (A) N2a cells cotransfected with LRPβ-myc and empty vector (lane 1) or ca-Src (lane 2) were immunoprecipitated with an anti-myc antibody and analyzed by immunoblotting with antibodies against phosphotyrosine, Src and the myc epitope. (B) N2a cells transfected with LRPβ-myc were immunostained with antibodies against the LRP-ICD (FITC, green) and phosphotyrosine (Cy3, red). (C) N2a cells were cotransfected with ca-Src or dn-Src and constructs encoding wild-type or LRPβ first or second NPXY motif mutants. Cells were immunostained as in (B), and the lifetime of FITC was determined by FLIM. Cy3 attached to a myc epitope at the C-terminus of wild-type LRPβ provided a positive FRET control. (D) Representative pseudocolored FLIM images representing average donor lifetimes on a pixel-by-pixel basis. Colors toward the red end of the spectrum indicate FRET. (*$p < 0.0001$ vs. no acceptor, dn-Src, and 2nd NPXY mutant conditions; **$p < 0.0001$ vs. no acceptor control).

in WI-38 cells after treatment with PDGF-BB by monitoring the lifetime of Alexa488 bound to the LRP-ICD in the presence of phosphotyrosine-bound Cy3 (Fig. 2A). We were able to show that PDGF induced a significant increase in LRP phosphorylation–measured as a decrease in Alexa488 lifetime–that was predictably small compared to the effect of Src transfection, given the fact that endogenous proteins and a more physiological stimulus were used. The small amount of "FRETing" molecules in the absence of stimulus points towards low-level baseline phosphorylation. The pseudocolored FLIM images revealed that phosphorylation of LRP did not affect the global LRP population as we observed with ca-Src transfection. Instead PDGF-BB treatment affected a morphologically distinct subpopulation of LRP, and only a subpopulation of LRP in small puncta near the cell surface appeared to be phosphorylated. This pattern indicates FRET in subdomains close to the cell surface and is in agreement with the finding the PDGF-induced phosphorylation (at least in fibroblasts) localizes to caveolae [6] and PDGF-r-β and LRP co-localize in clathrin coated pits [8]. Similar results were obtained in murine primary cortical neurons (Fig. 2B), indicating that stimulus-induced phosphorylation of LRP occurs at or near the cell surface in neurons as well. This is of specific interest since both PDGF and an inhibitor of PDGF-r signalling have recently been shown to influence APP processing [11–13].

PDGF-r-β and LRP interact as shown by co-immunoprecipitation, co-localization, and FRET measurements

Small molecule inhibitors of PDGF-r activation and Src activity prevent PDGF-induced phosphorylation of LRP [7]. Formation of a complex including the two recep-

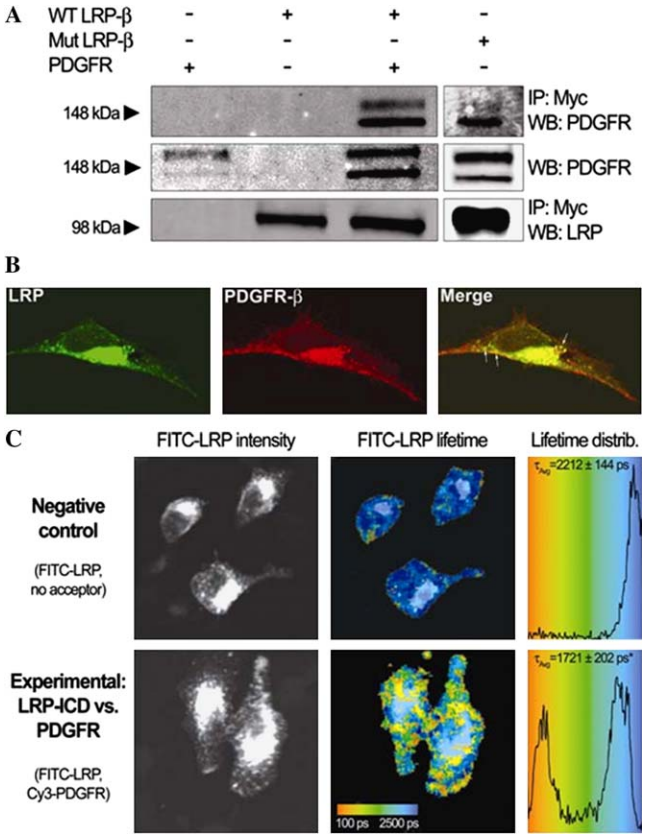

Fig. 3. PDGF-r-β coimmunoprecipitates, colocalizes, and FRETs with the LRP-ICD. N2a cells were cotransfected with LRPβ-myc and empty vector or PDGF-r-β and analyzed one day after transfection. Antibodies were against the intracellular domains of both proteins. (A) Lysates were immunoprecipitated with an antibody against the myc epitope and analyzed by immunoblotting. (B) LRPβ-myc was labeled with FITC and PDGF-r-β was labeled with Cy3 in cotransfected cells. (C) Cells were immunostained with FITC and Cy3 on the intracellular domains of LRP and PDGF-r-β, respectively. The lifetime of FITC was measured as described in Fig. 2 ($p < 0.0001$).

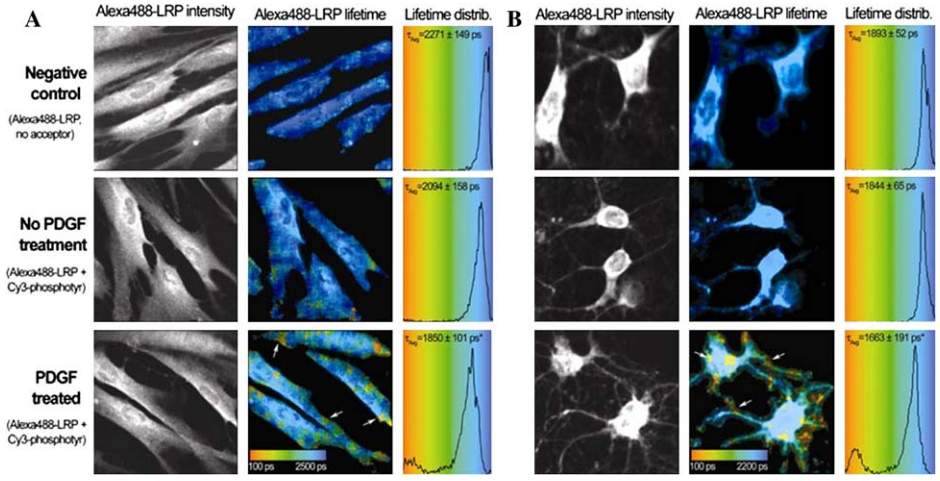

Fig. 2. PDGF-induced phosphorylation of endogenous LRP measured by FLIM. WI-38 cells (A) and primary neurons (B) were serum starved and incubated with 50 ng/ml PDGF-BB for 12 min. Cells were immunostained with Alexa488 on the LRP-ICD and Cy3 on phosphotyrosine residues. The lifetime of Alexa488 was determined as described in Fig. 2. Representative cells are shown in pseudocolored images, in which "FRETing" molecules appear in red and non"FRETing" molecules appear in blue. (Untreated vs. PDGF treated $p < 0.0001$ for both cell types.)

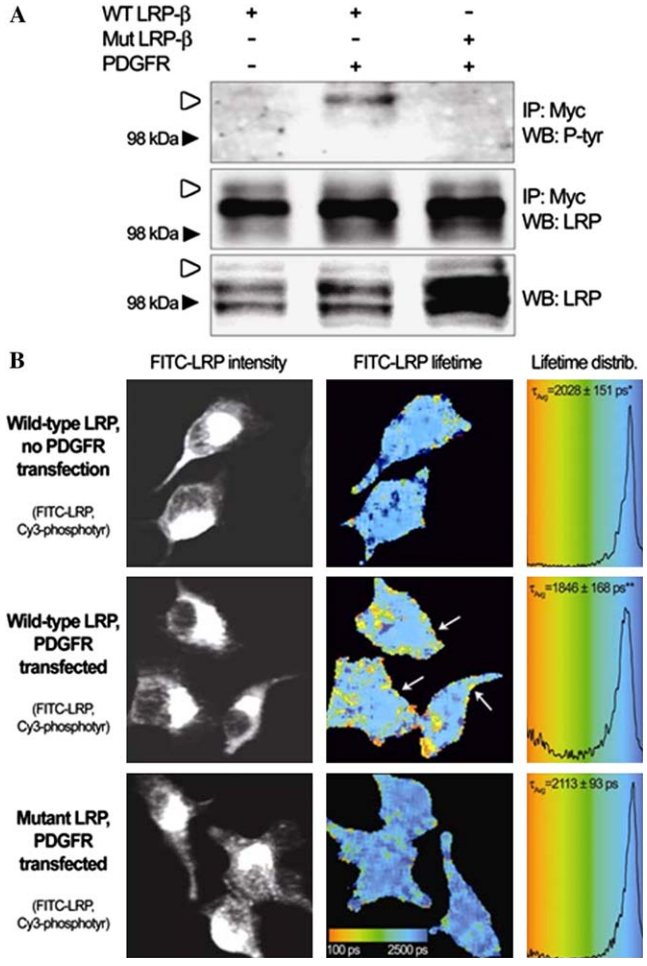

Fig. 4. Overexpression of PDGF-r-β results in phosphorylation of the LRP-ICD on Tyr63. N2a cells cotransfected with empty vector or PDGF-r-β and wild-type myc-LRPβ or the 2nd NPXY mutant were analyzed one day after transfection. (A) LRPβ was immunoprecipitated with antibodies against the myc epitope and analyzed by immunoblotting with antibodies against the myc epitope and phosphotyrosine. (B) Cells were immunostained with FITC and Cy3 on the LRP-ICD and phosphotyrosine, respectively. The lifetime of FITC was measured as described in Fig. 2.

tors would suggest a relatively short, direct signalling cascade, whereas the absence of a complex could imply a longer, more indirect chain of events leading to phosphorylation. We cotransfected wildtype myc-LRPβ or its second NPXY mutant with PDGF-r-β in N2a cells and confirmed that immunoprecipitation of LRPβ pulls down PDGF-r [3]. The interaction was not dependent on the integrity of LRP's second NPXY domain, indicating that the interaction is not dependent on tyrosine phosphorylation of LRP or binding of the second NPXY motif (Fig. 3A).

Cotransfected LRPβ and PDGF-r-β colocalize at the light level throughout the cell, with strong staining predominantly in perinuclear compartments and also at the cell surface (Fig. 3B). To determine whether their interaction has a more discrete subcellular localization in intact cells, we developed a FLIM assay in which the proximity of the LRP-ICD to the PDGF-r-β CT was assessed. As is shown in Fig. 3C, a distinct population of "FRET-ing" LRP-bound FITC was observed at or close to the cell-surface, whereas no FRET occurred in areas of high LRP concentration in the ER and Golgi. The distribution pattern and large difference in lifetime between the interacting and non-interacting populations is consistent with formation of a tight LRP/PDGF-r-β complex and complements the co-immunoprecipitation data suggesting that LRP and PDGF-r form a complex at or near the cell surface. Interestingly, LRPβ that was immunoprecipitated in the presence of overexpressed PDGF-r-β was phosphorylated without further stimulus if its distal NPXY domain was intact (Fig. 4A). LRP-ICD phosphorylation detected by FLIM under these conditions existed in patches at the cell surface resembling that caused by PDGF-BB stimulus and distinct from the even cell-surface phosphorylation induced by ca-Src (Fig. 4B). These findings suggest that PDGF-r overexpression induces dimerization and autophosphorylation of PDGF-r-β in a manner similar to PDGF-BB treatment [8].

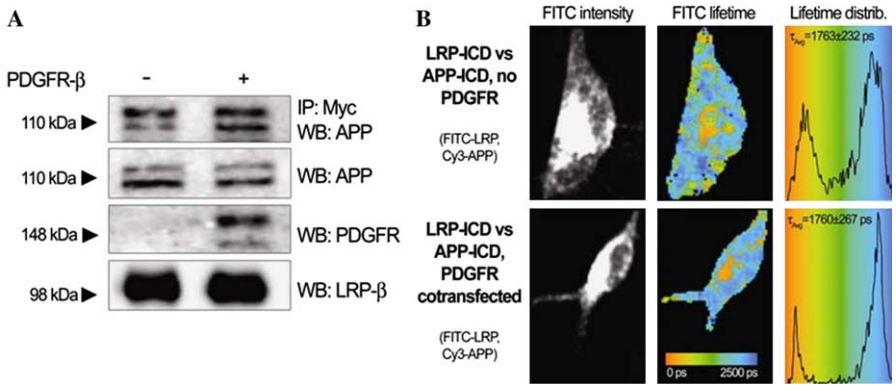

Fig. 5. Caveolar phosphorylation of LRP does not alter proximity to APP695. N2a cells were cotransfected with LRPβ-myc, APP695-V5, and either empty vector or PDGF-r-β. (A) Lysates were immunoprecipitated with an antibody against the myc epitope and analyzed by immunoblotting. (B) Cells were immunostained with FITC and Cy3 on the intracellular domains of LRP and APP, respectively. The lifetime of FITC was measured as described in Fig. 2.

LRP induced phosphorylation by PDGF-r overexpression does not alter APP–LRP interaction

Since both PDGF and an inhibitor of PDGF-r signalling have recently been shown to influence APP processing [11–13] we examined whether phosphorylation of LRP changed its interaction with APP. To isolate this NPXY domain mediated interaction from the KPI mediated APP–LRP binding interaction, we used the APP695 isoform that predominates in neurons and does not contain the KPI domain containing exons. In co-immunoprecipitation experiments, the presence of PDGF-r did not influence the strength of the C-terminal mediated interaction of LRP with APP695 (Fig. 5A). Since APP695 and LRP exhibit intracellular interactions in the ER/Golgi in addition to the cell surface, though, the effect of phosphorylating LRP at or near the cell-surface might not be revealed in Co-IP experiments. Measuring FRET between the C-termini of APP695 and LRP using FLIM allowed direct comparison of the interaction in both regions of the cell (Fig. 5B). PDGF-r overexpression did not change either total or subcellular (near the cell surface) LRP–APP695 interactions.

In this study, we developed multiphoton time domain FLIM as a technique for monitoring the subcellular distribution of specific post-translational modifications of endogenous proteins. Phosphorylation of the carboxyl tail of LRP was observed after stimulation of tyrosine kinase activity using constitutively active Src, in a different pattern than that observed by PDGF-r-β transfection, or stimulation of endogenous PDGF-r with its native ligand, PDGF-BB. Constitutive Src activation affected most if not all cellular LRP. Cytokine treatment, however, induced phosphorylation of a subpopulation of LRP that localized to the periphery of the cell, possibly in caveolae-like subdomains or newly formed endosomal compartments. Importantly, stimulus-induced phosphorylation was also observed on endogenous LRP in cultured neurons. In comparison to traditional techniques, this FRET based approach adds spatial resolution to immunoprecipitation/Western blot approaches. Raising unique antibodies to specific phosphoepitopes is difficult, especially for proteins in which the phosphorylation occurs in a common motif like an NPXY domain. Thus the FRET approach developed here utilizing FLIM may be broadly applicable to the issue of identifying the subcellular distribution of specific post-translational changes in overexpressed as well as endogenous protein targets like LRP with exquisite spatial resolution.

Acknowledgments

This work was supported by National Institutes of Health Grant AG12406 and research fellowships from the Deutsche Forschungsgemeinschaft to AVT (TH 1129/1-1) and CVA (AR379/1-1). We thank Michelle Tangredi and Dr. Robert Spoelgen for invaluable advice.

References

[1] G.W. Rebeck, J.S. Reiter, D.K. Strickland, B.T. Hyman, Apolipoprotein E in sporadic Alzheimer's disease: allelic variation and receptor interactions, Neuron 11 (1993) 575–580.
[2] J. Herz, D.K. Strickland, LRP: a multifunctional scavenger and signaling receptor, J. Clin. Invest. 108 (2001) 779–784.
[3] P. Boucher, M. Gotthardt, W.P. Li, R.G. Anderson, J. Herz, LRP: role in vascular wall integrity and protection from atherosclerosis, Science 300 (2003) 329–332.
[4] D.K. Swertfeger, G. Bu, D.Y. Hui, Low density lipoprotein receptor-related protein mediates apolipoprotein E inhibition of smooth muscle cell migration, J. Biol. Chem. 277 (2002) 4141–4146.
[5] Y. Zhu, D.Y. Hui, Apolipoprotein E binding to low density lipoprotein receptor-related protein-1 inhibits cell migration via activation of cAMP-dependent protein kinase A, J. Biol. Chem. 278 (2003) 36257–36263.
[6] P. Boucher, P. Liu, M. Gotthardt, T. Hiesberger, R.G. Anderson, J. Herz, Platelet-derived growth factor mediates tyrosine phosphorylation of the cytoplasmic domain of the low density lipoprotein receptor-related protein in caveolae, J. Biol. Chem. 277 (2002) 15507–15513.
[7] E. Loukinova, S. Ranganathan, S. Kuznetsov, N. Gorlatova, M.M. Migliorini, D. Loukinov, P.G. Ulery, I. Mikhailenko, D.A. Lawrence, D.K. Strickland, Platelet-derived growth factor (PDGF)-induced tyrosine phosphorylation of the low density lipoprotein receptor-related protein (LRP). Evidence for integrated co-receptor function between LRP and the PDGF, J. Biol. Chem. 277 (2002) 15499–15506.
[8] C.S. Newton, E. Loukinova, I. Mikhailenko, S. Ranganathan, Y. Gao, C. Haudenschild, D.K. Strickland, Platelet-derived growth factor receptor-β (PDGF-r-β) activation promotes its association with the low density lipoprotein receptor-related protein (LRP). Evidence for co-receptor function, J. Biol. Chem. 280 (2005) 27872–27878.
[9] A. Kinoshita, C.M. Whelan, C.J. Smith, I. Mikhailenko, G.W. Rebeck, D.K. Strickland, B.T. Hyman, Demonstration by fluorescence resonance energy transfer of two sites of interaction between the low-density lipoprotein receptor-related protein and the amyloid precursor protein: role of the intracellular adapter protein Fe65, J. Neurosci. 21 (2001) 8354–8361.
[10] S. Ranganathan, C.X. Liu, M.M. Migliorini, C.A. Von Arnim, I.D. Peltan, I. Mikhailenko, B.T. Hyman, D.K. Strickland, Serine and threonine phosphorylation of the low density lipoprotein receptor-related protein by protein kinase Cralpha regulates endocytosis and association with adaptor molecules, J. Biol. Chem. 279 (2004) 40536–40544.
[11] D. Gianni, N. Zambrano, M. Bimonte, G. Minopoli, L. Mercken, F. Talamo, A. Scaloni, T. Russo, Platelet-derived growth factor induces the β-γ-secretase-mediated cleavage of Alzheimer's amyloid precursor protein through a Src-Rac-dependent pathway, J. Biol. Chem. 278 (2003) 9290–9297.
[12] C. Kim, C.H. Jang, J.H. Bang, M.W. Jung, I. Joo, S.U. Kim, I. Mook-Jung, Amyloid precursor protein processing is separately regulated by protein kinase C and tyrosine kinase in human astrocytes, Neurosci. Lett. 324 (2002) 185–188.
[13] W.J. Netzer, F. Dou, D. Cai, D. Veach, S. Jean, Y. Li, W.G. Bornmann, B. Clarkson, H. Xu, P. Greengard, Gleevec inhibits β-amyloid production but not notch cleavage, Proc. Natl. Acad. Sci. USA 100 (2003) 12444–12449.
[14] I. Mikhailenko, F.D. Battey, M. Migliorini, J.F. Ruiz, K. Argraves, M. Moayeri, D.K. Strickland, Recognition of ralpha2-macroglobulin by the low density lipoprotein receptor-related protein requires the cooperation of two ligand binding cluster regions, J. Biol. Chem. 276 (2001) 39484–39491.
[15] O. Berezovska, P. Ramdya, J. Skoch, M.S. Wolfe, B.J. Bacskai, B.T. Hyman, Amyloid precursor protein associates with a nicastrin-dependent docking site on the presenilin 1-γ-secretase complex in

cells demonstrated by fluorescence lifetime imaging, J. Neurosci. 23 (2003) 4560–4566.
[16] M.Q. Xia, B.J. Bacskai, R.B. Knowles, S.X. Qin, B.T. Hyman, Expression of the chemokine receptor CXCR3 on neurons and the elevated expression of its ligand IP-10 in reactive astrocytes: in vitro ERK1/2 activation and role in Alzheimer's disease, J. Neuroimmunol. 108 (2000) 227–235.
[17] B.J. Bacskai, J. Skoch, G.A. Hickey, R. Allen, B.T. Hyman, Fluorescence resonance energy transfer determinations using multiphoton fluorescence lifetime imaging microscopy to characterize amyloid-β plaques, J. Biomed. Opt. 8 (2003) 368–375.
[18] T. Ng, A. Squire, G. Hansra, F. Bornancin, C. Prevostel, A. Hanby, W. Harris, D. Barnes, S. Schmidt, H. Mellor, P.I. Bastiaens, P.J. Parker, Imaging protein kinase C α activation in cells, Science 283 (1999) 2085–2089.
[19] H. Barnes, E.J. Ackermann, P. van der Geer, v-Src induces Shc binding to tyrosine 63 in the cytoplasmic domain of the LDL receptor-related protein 1, Oncogene 22 (2003) 3589–3597.
[20] Y. Li, J. Cam, G. Bu, Low-density lipoprotein receptor family: endocytosis and signal transduction, Mol. Neurobiol. 23 (2001) 53–67.
[21] M. Yang, H. Huang, J. Li, D. Li, H. Wang, Tyrosine phosphorylation of the LDL receptor-related protein (LRP) and activation of the ERK pathway are required for connective tissue growth factor to potentiate myofibroblast differentiation, Faseb J. 18 (2004) 1920–1921.